Preclinical Activity of PI3K Inhibitor Copanlisib in Gastrointestinal Stromal Tumor

Alfonso García-Valverde[1], Jordi Rosell[1], Garazi Serna[2], Claudia Valverde[3], Joan Carles[3], Paolo Nuciforo[2], Jonathan A. Fletcher[4], Joaquín Arribas[5,6], Oliver Politz[7], and César Serrano[1,3]

ABSTRACT

KIT or PDGFRA gain-of-function mutations are the primary drivers of gastrointestinal stromal tumor (GIST) growth and progression throughout the disease course. The PI3K/mTOR pathway is critically involved in the transduction of KIT/PDGFRA oncogenic signaling regardless of the type of primary and secondary mutations, and therefore emerges as a relevant targetable node in GIST biology. We evaluated in GIST preclinical models the antitumor activity of copanlisib, a novel pan-class-I PI3K inhibitor with predominant activity against p110α and p110δ isoforms, as single-agent and in combination with first-line KIT inhibitor imatinib. *In vitro* studies undertaken in one imatinib-sensitive (GIST-T1) and two imatinib-resistant (GIST-T1/670 and GIST430/654) GIST cell models showed that single-agent copanlisib effectively suppressed PI3K pathway activation leading to decreased cell viability and proliferation in both imatinib-sensitive and -resistant cells irrespective of the type of primary or secondary KIT mutations. Simultaneous PI3K and KIT inhibition with copanlisib and imatinib resulted in enhanced impairment of cell viability in both imatinib-sensitive and -resistant GIST cell models, although apoptosis was mostly triggered in GIST-T1. Single-agent copanlisib inhibited GIST growth *in vivo*, and conjoined inhibition of PI3K and KIT was the most active therapeutic intervention in imatinib-sensitive GIST-T1 xenografts. IHC stain for cleaved-caspase 3 and phospho-S6 support a predominant antiproliferative effect of copanlisib in GIST. In conclusion, copanlisib has single-agent antitumor activity in GIST regardless KIT mutational status or sensitivity to imatinib. Effective KIT inhibition is necessary to achieve synergistic or additive effects with the combination of imatinib and any given PI3K/mTOR pathway inhibition.

Introduction

Gastrointestinal stromal tumor (GIST) is the most common malignant mesenchymal neoplasm (1, 2) and is primarily defined by oncogenic, gain-of-function mutations in the KIT or platelet-derived growth factor receptor alpha (PDGFRA) receptor tyrosine kinases (RTK), which are present in 85%–90% of patients with GIST (3, 4). Oncogenic addiction to KIT signaling is essential throughout GIST development and tumor evolution (4, 5) and KIT inhibition with first-line tyrosine kinase inhibitor (TKI) imatinib mesylate leads to substantial clinical benefit in advanced or metastatic GIST (6). Resistance to imatinib eventually occurs in most patients and entails reactivation of KIT receptor and KIT downstream pathways due to positive selection of clones with acquired secondary mutations in KIT, which constitutes the main mechanism of failure to imatinib in 80%–90% of patients with GIST (7). Although TKIs with KIT inhibitory activity such as sunitinib and regorafenib are approved in the second- and the third-line of treatment, respectively, their benefit is modest (5, 8, 9) because the structural heterogeneity of the different KIT/PDGFRA oncoproteins complicates the design of drugs that could effectively inhibit all mutant RTKs. Therefore, novel treatment strategies are needed.

Importantly, KIT/PDGFRA oncogenic signaling is mainly driven by PI3K/mTOR and RAS/MAPK pathways through direct interaction with PI3K and GRB2 signaling intermediates, which occurs irrespective of whether the particular KIT/PDGFRA mutations are imatinib sensitive or imatinib resistant (10–12). Specifically, KIT-activated PI3K/mTOR pathway is crucial in GIST tumor initiation, development, and survival (13). Furthermore, early preclinical studies demonstrated strong antiproliferative and proapoptotic effects upon PI3K inhibition in imatinib-sensitive and -resistant GIST models, both as monotherapy and in combination with imatinib (10–15), thereby emerging as appealing therapeutic strategies. However, subsequent clinical trials achieved scarce clinical benefit or are yet to be reported (5, 16–18).

Copanlisib (Bayer AG) is a novel potent pan-class I PI3K inhibitor with predominant activity against p110α and p110δ PI3K isoforms (19). Preclinical studies demonstrated consistent antiproliferative activity and apoptosis induction in several cancer models, and early clinical trials have shown meaningful activity in patients with both solid tumors and hematologic malignancies (20–25). Recently, copanlisib was approved by FDA for the treatment of relapsed follicular lymphoma.

In this study we evaluated *in vitro* and *in vivo* the antitumor activity of copanlisib as single-agent and in combination with first-line imatinib using a panel of human GIST cells lines with clinically representative primary and secondary KIT mutations.

[1]Sarcoma Translational Research Laboratory, Vall d'Hebron Institute of Oncology (VHIO), Barcelona, Spain. [2]Molecular Oncology Laboratory, Vall d'Hebron Institute of Oncology (VHIO), Barcelona, Spain. [3]Department of Medical Oncology, Vall d'Hebron University Hospital, Barcelona, Spain. [4]Department of Pathology, Brigham and Women's Hospital and Harvard Medical School, Boston, Massachusetts. [5]Institució Catalana de Recerca I Estudis Avançats (ICREA), Barcelona, Spain. [6]Preclinical Research Program, Vall d'Hebron Institute of Oncology (VHIO), Barcelona, Spain. [7]Bayer AG, Preclinical Research Oncology, Berlin, Germany.

Note: Supplementary data for this article are available at Molecular Cancer Therapeutics Online (http://mct.aacrjournals.org/).

J. Arribas and C. Serrano contributed equally as co-senior authors of this article.

Corresponding Author: César Serrano, Hospital Universitario Vall d'Hebron, Passeig Vall d'Hebron 119, Barcelona 08035, Spain. Phone: 349-3254-3450; Fax: 349-3489-4015; E-mail: cserrano@vhio.net

Mol Cancer Ther 2020;19:1289–97

doi: 10.1158/1535-7163.MCT-19-1069

Materials and Methods

Cell lines

GIST-T1 is a primary GIST cell line with a heterozygous activating mutation in *KIT* exon 11 (Val560_Tyr578del) established from a metastasis of a patient with untreated GIST. GIST-T1/670 is a subcell line of GIST-T1 with a secondary mutation in *KIT* exon 14 (T670I) that was established by selective pressure with imatinib. GIST430/654 is a primary GIST cell line with a *KIT* primary heterozygous exon 11 in-frame deletion and a *KIT* heterozygous exon 13 missense-resistant mutation (V654A), established from a patient that had progressed to imatinib. Cells were grown as described previously (26). All lines were credentialed by Sanger sequencing evaluations of known mutations, at baseline and every 3 months during the study. All cultures were shown to be *Mycoplasma* free.

Reagents

Imatinib mesylate was purchased from LC Laboratories and copanlisib was provided by Bayer AG.

Viability assays

Cell viability studies were carried out using Cell Titer-Glo luminescent assay from Promega, in which the luciferase catalyzed luciferin/ATP reaction provides an indicator of cell number. For these studies, cell lines were plated in triplicates at 5,000 (GIST-T1 and GIST-T1/670) and 10,000 (GIST430/654) cells per well in a 96-well flat-bottomed plate (Falcon), and then incubated for 3 (GIST-T1 and GIST-T1/670) or 6 days (GIST430/654) with imatinib and copanlisib at different concentrations or DMSO. The Cell Titer-Glo assay luminescence was measured with Infinite 200 Pro Microplate Luminometer (Tecan Trading AG) and the data were normalized to the DMSO control group.

5-Bromodeoxyuridine assay

Cell proliferation studies were carried out using BrdU Cell Proliferation ELISA Assay (Roche) according to the manufacturer's protocol. For these studies, cell lines were seeded in triplicates at 10,000 (GIST-T1 and GIST-T1/670) and 15,000 (GIST430/654) cells per well in a 96-well tissue culture plate (Sigma-Aldrich) and were incubated in media containing drugs and DMSO for 48 hours. 5-bromodeoxyuridine (BrdU) was added and incubation was continued for 24 hours. Assay plates were measured with Infinite 200 Pro Microplate Luminometer (Tecan Trading AG).

Apoptosis induction assay

Apoptosis induction studies were performed by measuring caspase-3 and caspase-7 activity with the Caspase-Glo 3/7 Assay Kit (Promega) according to the manufacturer's protocol. Cells were plated in triplicates in 96-well flat-bottomed plates at 5,000 (GIST-T1 and GIST-T1/670) and 10,000 (GIST430/654) cells per well. After 24-hour culture, medium was replaced with fresh medium (with or without respective drugs) and apoptosis was measured according to the manufacturer's instructions at 24 (GIST-T1 and GIST-T1/670) and at 48 hours (GIST430/654) with Infinite 200 Pro Microplate Luminometer (Tecan Trading AG).

Western blot assays

Preparation of whole-cell lysates was done as described previously (26). Electrophoresis was carried out in 10% polyacrylamide gels and transferred to nitrocellulose membranes. Bands were detected by incubating with Immobilon Forte Western HRP Substrate (Millipore-MERK KGaA) and captured by chemiluminescence with Amersham Imager 600 (GE Healthcare Life Science).

Primary antibodies to phospho-KIT Y703 (#3073), phospho-AKT S473 (#9271), total AKT (#9272), S6RP (#2317), phospho-S6 S235/6 (#2211), phospho-ERK Thr202/Tyr204 (#9101) and total ERK (#9102), and cleaved-PARP Asp214 (#9541) were from Cell Signaling Technology; to total KIT (A4502) was from Dako; and to Cyclin A (sc-751) was from Santa Cruz Biotechnology.

GIST xenograft studies

Six- to 8-week-old female athymic nude mice (NMRI Foxn1/nu-Fosn1/nu) were obtained from Janvier Laboratories and housed under specific pathogen-free conditions. Heterotopic GIST xenografts were generated by subcutaneous injection of GIST-T1 and GIST-T1/670 [5×10^6 cells in culture medium and Matrigel (Cultek SL) at 1:1 ratio] in anesthetized animals (ketamine 100 mg/kg i.p. and xylacine 10 mg/kg i.p.). Animals were maintained at $22 \pm 2°C$ and 35% humidity, on a 12-hour light-dark cycle. An individually positive pressure ventilated cage system was used to house a maximum of 5 mice per cage. Food and water were provided *ad libitum*. All animal studies were performed in accordance with ARRIVE guidelines and the three Rs rule of replacement, reduction, and refinement principles. All *in vivo* work was conducted under appropriate Institutional Animal Care and Use Committee approved protocols.

Mice were randomized into the following treatment arms when median tumor volume reached 200 mm^3: control group, copanlisib (14 mg/kg, i.v./3 times weekly, t.i.w), imatinib (100 mg/kg orally/every day), and the combination of copanlisib and imatinib (Supplementary Table S1). Solvents for imatinib and copanlisib were sterile water and 5% D-Mannitol in sterile water, respectively. Tumor volume and animal weight were assessed 3 times a week. Animals were euthanized after 21 days of treatment or when tumor volume reached 1,200 mm^3. Tumors were collected and fixed in 4% buffered formaldehyde for further histologic analysis. Blood was collected at day 21, 4 hours after drug administration through intracardiac puncture. Plasma was obtained by centrifugation and frozen down for further pharmacokinetic analysis.

IHC analysis

Tumor samples were collected 4 hours after last drug administration and immediately fixed in fresh 4% paraformaldehyde at 4°C overnight. After paraffin embedding, viable areas from single hematoxylin and eosin slides were selected to generate tumor microarrays containing two 1.0-mm cores per case. IHC staining antibodies used were Phospho-S6 Ribosomal Protein Ser235/6 (dilution 1:400; #2211), Cleaved Caspase-3 Asp175 (dilution 1:200; #9661), phospho-4EBP1 Thr70 (dilution 1:75; #9455), and phospho-AKT Ser473 (dilution 1:100; #4060) from Cell Signaling Technology and total KIT (dilution 1:400; A4502) from Dako. Slides were digitalized at 20× using the NanoZoomer 2.0HT (Hamamatsu Photonics). Digitalized images were uploaded into VISIOPHARM (VIS) Image Analysis Software (Visiopharm Integrator System version 2019.02.1.6005, Visiopharm) for the analysis. Custom-developed algorithms were created for each of the biomarkers with the supervision of a pathologist using the author module. Two color-deconvolution bands are used as preprocessing steps to enhance tissue and stained regions. The classification of the stained (positive) and nonstained (negative) region is based on an intensity-based thresholding classifier. The classifier segments the tissue into two parts: stained and nonstained. The output variables obtained from these protocols include the total area, stained area, and

the percentage of stained area, which was used for the analysis. Regarding IHC analysis, each case is the result of the average from two independent samples measurements per mice. A group average ± the SEM was used to build the graphics and perform the statistical analysis.

Pharmacokinetic studies

Plasma samples were thawed at room temperature. Within 30 minutes samples were mixed by inversion and, if necessary, centrifuged at room temperature for about 10 seconds at 3,000 × *g* to remove precipitates. After protein removal, samples were analyzed by high-performance liquid chromatography coupled with a tandem mass spectrometer (Applied Biosystems MDS Sciex API 6500) using the internal standard method. Measurement was performed with calibration samples, quality control samples, and unknown samples.

Statistical analysis

Differences between different treatment groups were analyzed with one-way ANOVA followed by a Holm–Sidak and Turkey multiple comparisons test. Differences with a $P \leq 0.05$ were considered to be significant. Statistical analysis was performed with GraphPad Prism version 6.0 (GraphPad Software, Inc.).

Results

Copanlisib inhibits PI3K in imatinib-sensitive and imatinib-resistant GIST cell lines

To assess the activity of copanlisib, we determined impact on cell growth and KIT-dependent signaling using GIST cell lines with clinically relevant mutations, representing imatinib-sensitive (GIST-T1) and imatinib-resistant disease (GIST430/654 and GIST-T1/670). Cell viability studies demonstrated that copanlisib was active in all GIST cell lines irrespective of KIT mutational status, showing IC_{50}s within the nanomolar range: 54.5 nmol/L (GIST-T1), 278.8 nmol/L (GIST-T1/670), and 78.7 nmol/L (GIST430/654; **Fig. 1A–C**; Supplementary Table S2). Proliferation studies with BrdU incorporation confirmed the antiproliferative effects of copanlisib in the same cell lines (**Fig. 1D–F**; Supplementary Table S2). These *in vitro* concentration ranges for efficacy correspond to levels relevant for clinical efficacy (23). The observed imatinib activity was within previously reported ranges (26).

Copanlisib inhibition of PI3K was evidenced in all GIST cell lines by suppression or significant reduction in the phosphorylation of KIT downstream PI3K targets AKT and S6-RP in comparison with DMSO-treated cells (**Fig. 2**). A decrease in the proliferation marker Cyclin A was observed between 24–48 hours depending on the cell line. In contrast, little to no induction of apoptosis monitored by cleaved PARP was detected, irrespective of the sensitivity to imatinib. Strong efficacy of copanlisib combined with induction of apoptosis was reported to be associated with a transient inhibition of pERK and a rebound after 24 hours, which is only seen here in the imatinib-sensitive cell line (GIST-T1; ref. 27).

Combined inhibition of PI3K and KIT with copanlisib and imatinib reduces cell viability irrespective of KIT mutation, but induces apoptosis only in imatinib-sensitive GIST

GIST cell lines were exposed to imatinib and increasing concentrations of copanlisib to determine the consequences of directly targeting both PI3K and KIT. The combination of copanlisib and imatinib achieved greater impairment in cell viability in both imatinib-sensitive and imatinib-resistant GIST cell lines compared with each drug alone, particularly at copanlisib concentrations of ≥100 nmol/L (**Fig. 3A–C**; Supplementary Table S3). A trend toward synergistic activity could be observed in all the three cell lines (ref. 28; Supplementary Table S4). Apoptosis induction with single-agent copanlisib was minimal and was only substantially induced in imatinib-sensitive cell line GIST-T1 upon concomitant KIT inhibition with imatinib (**Fig. 3D**), but not in the imatinib-resistant cell models (**Fig. 3E** and **F**).

Kinase inhibition studies (**Fig. 2**) demonstrated that combined inhibition of PI3K and KIT led to further PI3K/AKT pathway blockage, as shown by more pronounced reduction in S6-RP phosphorylation compared with copanlisib alone, particularly in GIST-T1/670 (**Fig. 2B**). Consistent with cell viability and apoptosis studies, simultaneous inhibition of PI3K and KIT with copanlisib and imatinib resulted in decreased proliferation, as shown by Cyclin A immunostaining, while PARP cleavage was more evident only in GIST-T1 (**Fig. 2A**), albeit at levels similar to those induced by imatinib in monotherapy.

In vivo activity of copanlisib as single-agent and in combination with imatinib

On the basis of the *in vitro* characterization of copanlisib as single agent or in combination with imatinib, we further explored *in vivo* the benefit of inhibiting PI3K alone or together with KIT inhibition. Heterotopic subcutaneous GIST xenografts were established using imatinib-sensitive (GIST-T1; $n = 27$) and imatinib-resistant (GIST-T1/670; $n = 18$) GIST cell lines (Supplementary Table S1) and randomized into four treatment arms at the previously indicated doses: vehicle; copanlisib; imatinib; and copanlisib and imatinib. Single-agent copanlisib significantly delayed tumor growth compared with vehicle in both GIST-T1 (**Fig. 4A**) and GIST-T1/670 (**Fig. 4D**) xenografts, as measured by tumor weight after 21 days of continuous treatment, when the study was terminated. As expected, imatinib significantly reduced tumor growth in the imatinib-sensitive GIST-T1 xenograft model ($P = < 0.001$), but not in the GIST-T1/670 model ($P = 0.135$). The combination of imatinib and copanlisib seemed to inhibit growth more than imatinib alone, but this was not a statistically significant difference ($P = 0.293$). No improvement was observed in GIST-T1/670 imatinib-resistant xenografts. Individual tumor volumes are displayed in Supplementary Fig. S1. Copanlisib levels in plasma samples obtained 4 hours after last drug administration at day 21 did not differ between GIST-T1 and GIST-T1/670, precluding pharmacokinetic effects as the basis for the differential activity (refs. 23, 29; Supplementary Fig. S2).

Potential IHC biomarkers of effective KIT downstream signaling inhibition with copanlisib and imatinib in GIST

In concordance with *in vitro* experiments, assessment of apoptosis induction by IHC expression of proapoptotic protein cleaved-caspase 3 revealed a significant increase in imatinib-sensitive GIST-T1 xenografts treated with copanlisib and imatinib compared with single-agent copanlisib, although no differences were observed with imatinib-induced apoptosis (**Fig. 4B**). In contrast, none of the treatments resulted in significant increase in cleaved-caspase 3 generation in GIST-T1/670 imatinib-resistant xenografts versus vehicle controls, also in agreement with *in vitro* results (**Fig. 4E**).

Among the various KIT downstream pathway biomarkers assessed by IHC *in vivo*, a decrease in serine 235/6 phosphorylation of S6-RP (compared with vehicle) tended to accompany antitumor activity of the different treatment conditions, thus indicating PI3K pathway modulation (**Fig. 4C** and **F**). None of remaining biomarkers tested (phosphorylation of AKT-Ser473, phosphorylation of 4EBP1-Thr70,

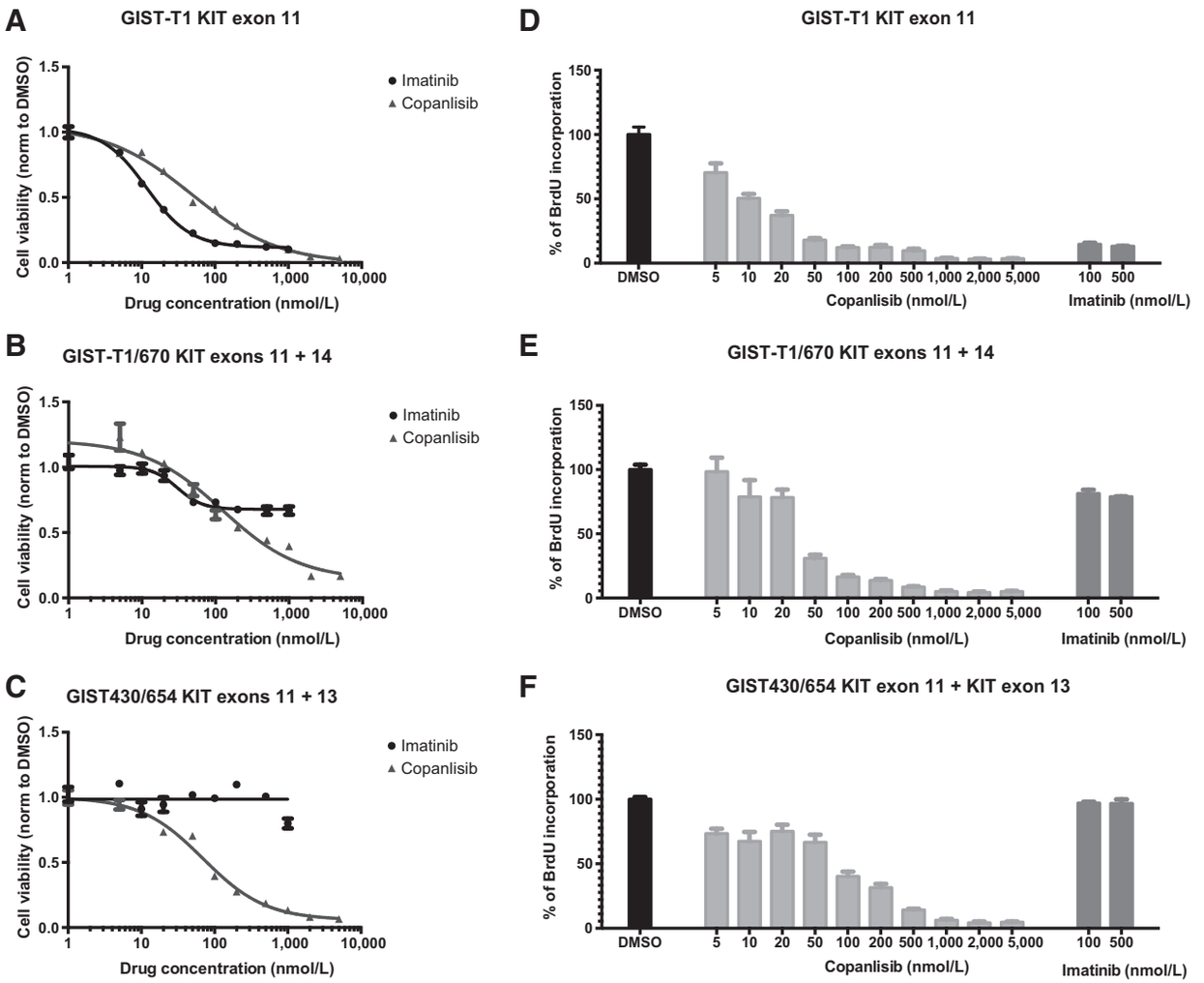

Figure 1.

In vitro antitumor activity of single-agent copanlisib versus imatinib in GIST cell lines. Cell viability was measured by Cell Titer-Glo assay in imatinib-sensitive GIST-T1 (**A**), and in imatinib-resistant GIST-T1/670 (**B**) and GIST430/654 (**C**). Proliferation was measured by BrdU incorporation in the same cell models: GIST-T1 (**D**), GIST-T1/670 (**E**), and GIST430/654 (**F**). All conditions were performed in triplicate. Norm, normalized to.

and total KIT expression) consistently reflected tumor behavior upon treatment (Supplementary Fig. S3). Representative positive stains for each marker are displayed in Supplementary Fig. S4. Together, these data support that copanlisib effect in GIST are mostly antiproliferative.

Discussion

Constitutive activation of PI3K/mTOR pathway through KIT/PDGFRA oncogenic signaling is indispensable for GIST development and maintenance of the GIST malignant phenotype (10, 11, 13). Accordingly, early studies based on targeted inhibition of PI3K highlighted PI3K/mTOR pathway essentiality in GIST based on the strong antiproliferative and proapoptotic effects achieved in both imatinib-sensitive and -resistant models (12, 14, 15, 30). These studies established the preclinical rationale that triggered the clinical development of several PI3K/mTOR pathway inhibitors either as single-agents or in combination with first-line KIT inhibitor, imatinib (16–18, 31, 32). Despite this solid preclinical rationale, prior PI3K/mTOR pathway inhibitors failed to show significant clinical activity in GIST. Copanlisib recently became one of only three PI3K inhibitors approved in cancer therapeutics from a plethora of PI3K antagonists investigated after nearly a decade of clinical research (24). Therefore, we studied copanlisib activity in imatinib-sensitive and -resistant GIST models with clinically representative KIT primary and secondary mutations.

Our studies demonstrate that copanlisib activity in GIST is mediated through specific abrogation of KIT downstream PI3K/mTOR signaling. PI3K inhibition with copanlisib as single-agent consistently leads to a predominant antiproliferative effect both *in vitro* and *in vivo* irrespective of the type of KIT primary or secondary mutation. Interestingly, apoptosis induction with copanlisib in monotherapy was modest in the imatinib-sensitive GIST-T1 cell line, and nearly absent in the imatinib-resistant cell models. Overall, this agrees not only with the delayed cell growth observed with PI3K inhibitor monotherapies in prior studies (12, 14, 15, 30), but also with the short-term disease stabilization and lack of major responses obtained

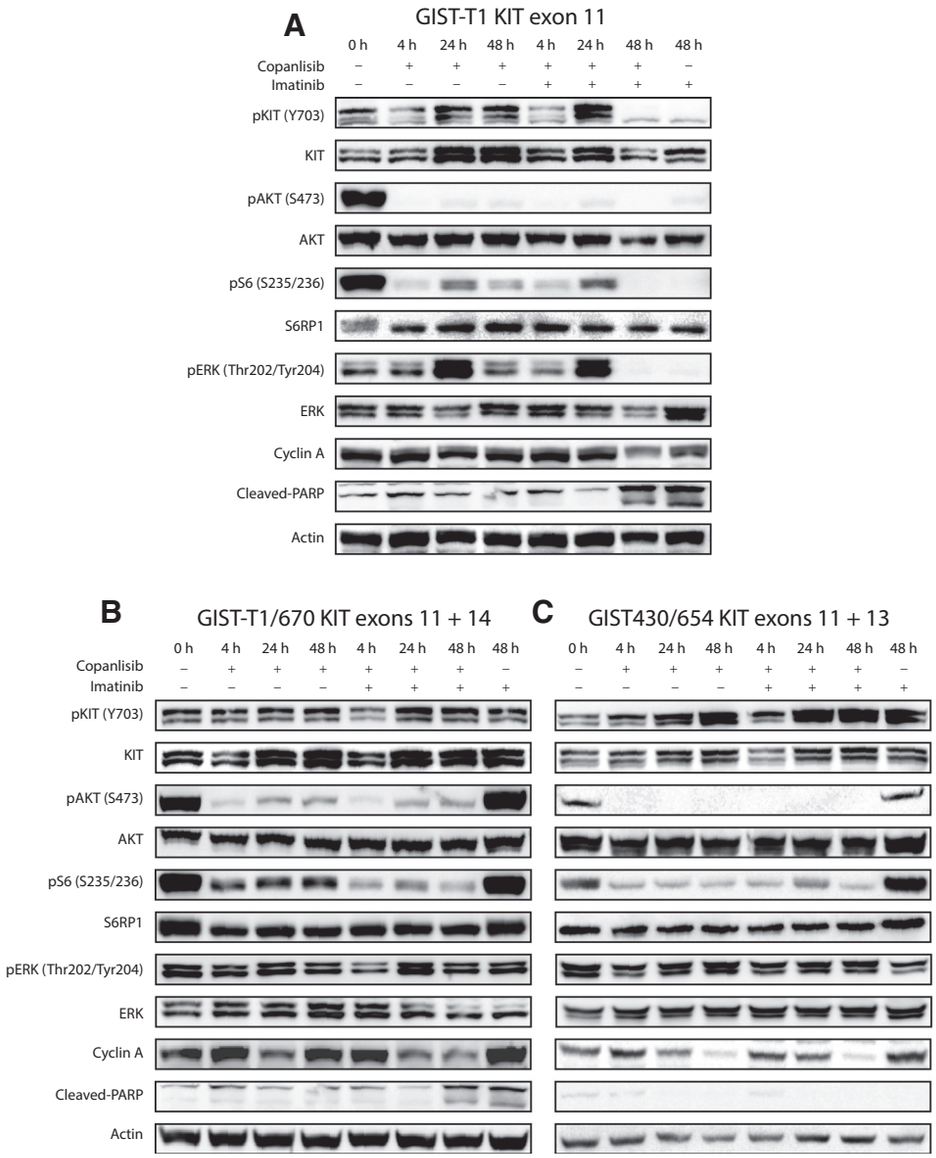

Figure 2.
PI3K pathway activation after incubation with copanlisib 200 nmol/L and/or imatinib 500 nmol/L for 4, 24, and 48 hours in GIST-T1 (**A**), GIST-T1/670 (**B**), and GIST430/654 (**C**).

with GDC-0980 in patients with imatinib-resistant GIST, the only PI3K/mTOR inhibitor for which clinical testing in GIST has been reported (16). Although previous preclinical studies underscored a major proapoptotic effect derived from PI3K pathway inhibition in GIST (12, 33), these early studies were largely performed with non-selective PI3K inhibitors (i.e.: LY294002). Therefore, it is possible that more focused targeting of the PI3K/mTOR pathway is insufficient to trigger apoptosis in the presence of activated KIT and KIT downstream RAS/MAPK signaling. Indeed, copanlisib effectiveness combined with apoptosis induction appears to be associated with transient inhibition of pERK in other RTK-driven models, which is only seen here in the imatinib-sensitive cell line (GIST-T1; ref. 27). Conversely, the lack of meaningful impact on MAPK signaling in the imatinib-resistant cell lines supports the relevance of this pathway and provides rationale for investigation of optimized combination strategies targeting both the PI3K and MAPK pathways in GIST. Together, copanlisib shows *in vitro* and *in vivo* antitumoral effect in GIST regardless the type of primary or secondary KIT mutation. This effect is largely mediated through inhibition of tumor proliferation.

In addition, we observed a previously unreported increase in total and phosphorylated KIT upon PI3K pathway inhibition, which was present at varying levels across all GIST models and paralleled MAPK pathway activation. There is a well-established positive feedback circuit where MAPK signaling downstream KIT stabilizes the ETV1 transcription factor, and ETV1 positively regulates KIT expression (34). Thus, it is conceivable that copanlisib-mediated phospho-ERK rebound (27) in the absence of meaningful transient inhibition fosters this feedback loop, which could contribute to the attenuated apoptotic response observed particularly in imatinib-resistant GIST. Further studies are needed to elucidate these aspects of GIST biology.

To potentiate tumor cell response, prior preclinical development focused on dual inhibition of oncogenic KIT signaling and the downstream PI3K/mTOR pathway, and several imatinib-based combinations targeting PI3K, AKT, and/or mTOR nodes were found to

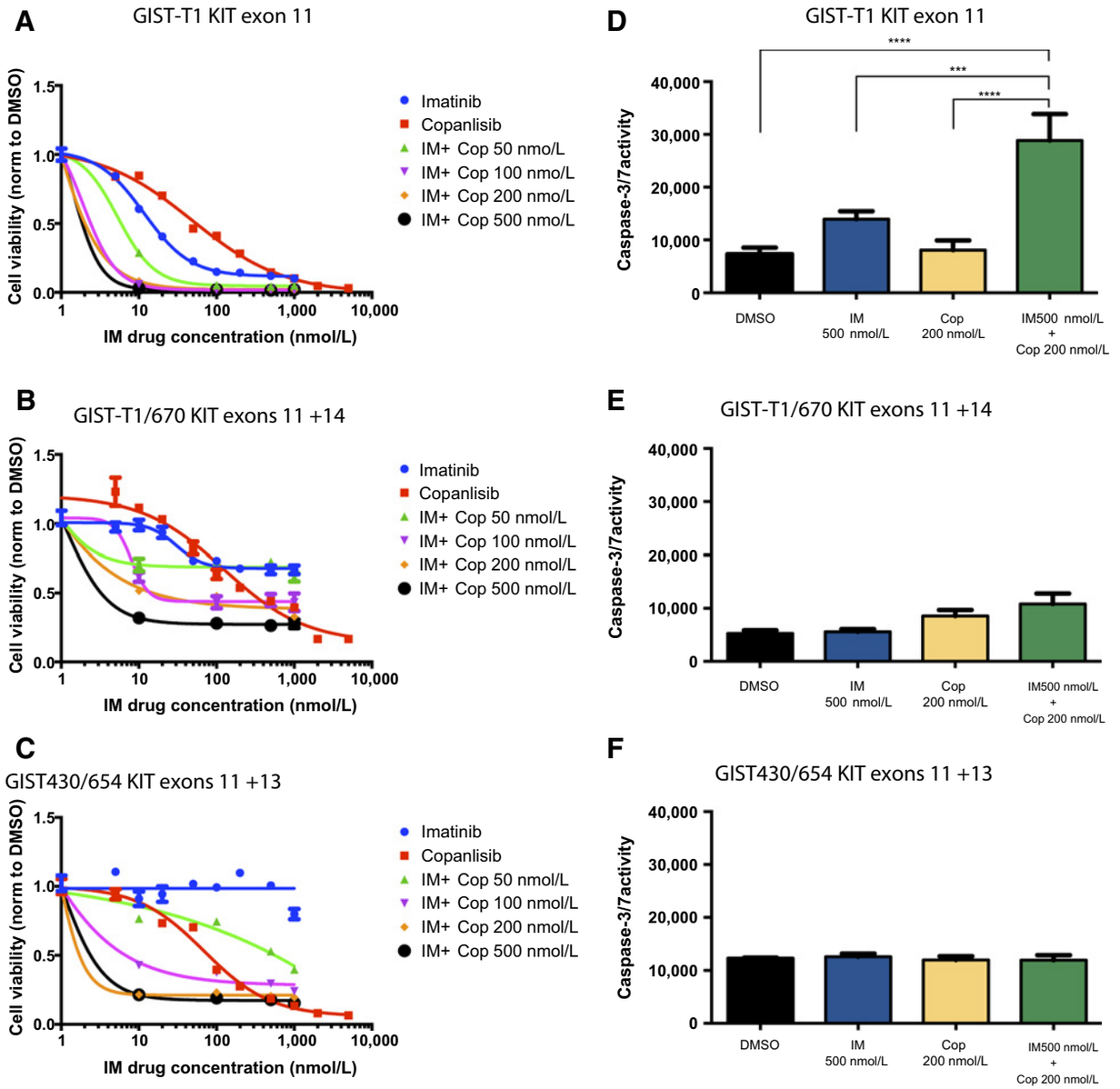

Figure 3.

In vitro antitumor activity of the combination of copanlisib and imatinib in GIST cell lines. Cell viability measured by Cell Titer-Glo assay after incubation with increasing doses of copanlisib (Cop), imatinib (IM), and copanlisib at concentrations of 50, 100, 200, and 500 nmol/L with increasing doses of imatinib, in GIST-T1 (**A**), GIST-T1/670 (**B**) and GIST430/654 (**C**). Apoptosis induction measured by caspase 3/7 activity in GIST cell lines after incubation of imatinib, copanlisib, or the combination of imatinib, in GIST-T1 (**D**), GIST-T1/670 (**E**), and GIST430/654 (**F**). All conditions were performed in triplicates. Differences between treatments were considered to be significant with a *P* value, * ≤ 0.05; ** ≤ 0.005; *** ≤ 0.001; **** ≤ 0.0001. Norm, normalized to; IM, imatinib; Cop, copanlisib.

significantly enhance the antitumor effects of KIT inhibition alone in both imatinib-sensitive and -resistant GIST cell models (12, 14, 15, 30). In agreement with prior studies, the imatinib and copanlisib combination achieved greater antiproliferative and apoptotic activity than either agent in monotherapy in the imatinib-sensitive model GIST-T1, resulting in *in vitro* and *in vivo* additive effects. Conversely, and unlike prior studies, the addition of imatinib to copanlisib in the two imatinib-resistant GIST cell models did not boost the antiproliferative effect achieved by single-agent copanlisib, nor its lack of apoptosis induction. These results are as accounted for by our observation that the KIT secondary mutations maintain substantial KIT oncogenic activity in the presence of imatinib. Thus, despite effective PI3K/mTOR pathway blockage, persistent upstream KIT signaling challenges the potential synergistic effects from the dual inhibition of KIT and PI3K/mTOR in imatinib-resistant GIST. In addition, GIST models used to evaluate *in vivo* the efficacy of imatinib plus PI3K inhibition may explain these discrepancies. GIST48 (also known as GIST48/820), a GIST cell line with a primary KIT mutation in exon 11, and a KIT secondary mutation in exon 17 (D820A), has been the only imatinib-resistant *in vivo* GIST model used in the past (14, 15). In contrast, we

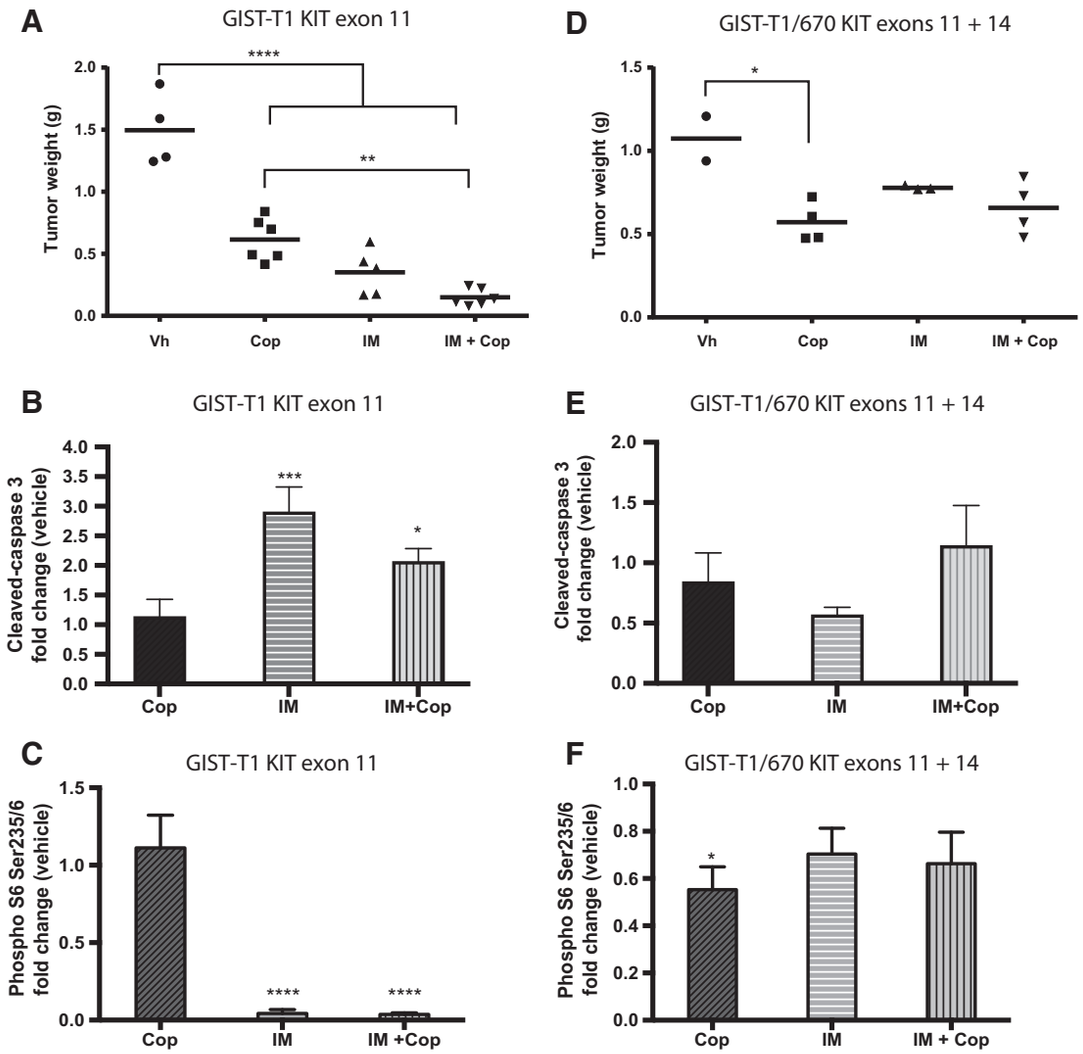

Figure 4.

In vivo antitumor activity of copanlisib (cop) as single-agent and in combination with imatinib (IM) in subcutaneous GIST xenografts with GIST-T1 and GIST-T1/670. Antitumor activity is expressed in tumor weight (g) at the endpoint (day 21) in GIST-T1 (**A**) and GIST-T1/670 (**D**). IHC analysis of caspase-3 expression in GIST-T1 (**B**) and GIST-T1/670 (**E**), and phosphorylation of S6RP-S235/6 in GIST-T1 (**C**) and GIST-T1/670 (**F**) are expressed as fold change normalized to vehicle (Vh). Differences between treatments was considered to be significant with a *P* value, * ≤ 0.05; ** ≤ 0.005; *** ≤ 0.001; **** ≤ 0.0001. IM, imatinib; Cop, copanlisib.

used GIST-T1/670, a GIST subline derived from GIST-T1 that harbors a primary KIT mutation in exon 11, and a KIT secondary mutation in exon 14 (T670I). Unlike GIST-T1/670, GIST48/820 appears to be partially sensitive to imatinib treatment (14, 15), something observed also in our hands, albeit *in vitro* (35). However, GIST-T1/670 is a GIST model that represents more substantially imatinib-resistant disease and predicts lack of synergistic or additive effect from the combination of imatinib and PI3K/mTOR pathways inhibitors in this setting. Congruently, such combinations have failed to demonstrate any clinical benefit in patients with GIST (16, 31, 32) or have never been reported (17, 18). Therefore, our studies highlight that inhibition of KIT oncogenic activation is critical to achieve additive or synergistic effects with dual KIT and PI3K targeting, thus first providing the molecular basis for prior trials failure in imatinib-resistance disease, and setting the field for novel combinations.

The polyclonal expansion of tumor subclones harboring heterogeneous KIT secondary mutations is the main mechanism of imatinib resistance in up to 90% of the patients (7). Arguably, prior trials investigating PI3K inhibition in GIST failed to show clinical activity due to the lack of oncogenic KIT signaling inhibition with imatinib in imatinib-resistant disease. Thus, as our results indicate the combination of imatinib and copanlisib would be only efficient in patients with imatinib-naïve GIST, although the excellent tolerability of imatinib hampers any investigation in the first-line. Interestingly, in the absence of approved TKIs with activity against the full spectrum of KIT secondary mutations (26), it is conceivable that broader abolition of imatinib-resistant KIT oncoproteins with the novel pan-KIT inhibitor ripretinib (36) might provide synergies with PI3K/mTOR pathway inhibition with copanlisib. This, instead, would have better chances of success in the clinical setting in patients with imatinib-resistant GIST. Alternatively, cojoined targeting of KIT downstream RAS/MAPK and

PI3K/mTOR pathways using novel creative drug schedules to minimize toxicity, may be a successful treatment strategy in imatinib-resistant disease.

Finally, IHC determination of cleaved-caspase 3 and the phosphorylation status of PI3K downstream effector S6 at serine 235/6 demonstrated consistency with *in vivo* treatment response in both GIST xenografts, overall supporting that copanlisib activity in GIST is mostly antiproliferative. Further clinical studies are warranted to explore this possibility. Potential feedback reactivation of AKT (37–39) and absence of well-validated AKT IHC antibodies likely hindered the assessment of AKT phosphorylation, a direct PI3K substrate, being not predictive of copanlisib activity in GIST models.

In conclusion, copanlisib has single-agent antitumor activity in GIST regardless KIT mutational status or sensitivity to imatinib, both *in vitro* and *in vivo*. Furthermore, our studies show that effective KIT inhibition is necessary to achieve synergistic or additive effects with the combination of imatinib and any given PI3K/mTOR pathway inhibition.

Disclosure of Potential Conflicts of Interest

J. Carles is a consultant (paid consultant) at Astellas, and has received speakers bureau honoraria from Bayer, Johnson & Johnson, Asofarma, and Astellas Pharma. J.A. Fletcher is a consultant (paid consultant) at Deciphera Pharmaceuticals. O. Politz is an employee (paid consultant) at Bayer AG. C. Serrano reports receiving a commercial research grant from Deciphera Pharmaceuticals, Pfizer, and Bayer AG, has received speakers bureau honoraria from Bayer and Blueprint Medicines, has an advisory board relationship with Deciphera Pharmaceuticals and Blueprint Medicines, and has provided expert testimony for Pharmamar, Pfizer, Bayer, Novartis, and Lilly. No potential conflicts of interest were disclosed by the other authors.

Authors' Contributions

Conception and design: A. García-Valverde, O. Politz, C. Serrano
Development of methodology: A. García-Valverde, J. Rosell, J.A. Fletcher, C. Serrano
Acquisition of data (provided animals, acquired and managed patients, provided facilities, etc.): A. García-Valverde, J. Rosell, G. Serna, P. Nuciforo, J.A. Fletcher, C. Serrano
Analysis and interpretation of data (e.g., statistical analysis, biostatistics, computational analysis): A. García-Valverde, G. Serna, C. Valverde, P. Nuciforo, J. Arribas, C. Serrano
Writing, review, and/or revision of the manuscript: A. García-Valverde, G. Serna, C. Valverde, J. Carles, P. Nuciforo, J. Arribas, O. Politz, C. Serrano
Administrative, technical, or material support (i.e., reporting or organizing data, constructing databases): J. Rosell, C. Serrano
Study supervision: O. Politz, C. Serrano

Acknowledgments

We express our gratitude to Dieter Zopf for being a critical reader of this article. This project was funded by a Bayer Research Grant (to C. Serrano).

The costs of publication of this article were defrayed in part by the payment of page charges. This article must therefore be hereby marked *advertisement* in accordance with 18 U.S.C. Section 1734 solely to indicate this fact.

Received November 20, 2019; revised February 23, 2020; accepted April 8, 2020; published first May 5, 2020.

References

1. Demetri GD, von Mehren M, Antonescu CR, DeMatteo RP, Ganjoo KN, Maki RG, et al. NCCN Task Force report: update on the management of patients with gastrointestinal stromal tumors. J Natl Compr Canc Netw 2010;2:S1–41.
2. Ducimetiére F, Lurkin A, Ranchére-Vince D, Decouvelaere A, Péoc'h M, Istier L, et al. Incidence of sarcoma histotypes and molecular subtypes in a prospective epidemiological study with central pathology review and molecular testing. PLoS One 2011;6:e20294.
3. Hirota S. Gain-of-function mutations of c-kit in human gastrointestinal stromal tumors. Science 1998;279:577–80.
4. Corless CL, Barnett CM, Heinrich MC. Gastrointestinal stromal tumours: origin and molecular oncology. Nat Rev Cancer 2011;11:865–78.
5. Serrano C, George S, Valverde C, Olivares D, García-Valverde A, Suárez C, et al. Novel insights into the treatment of imatinib-resistant gastrointestinal stromal tumors. Target Oncol 2017;12:277–88.
6. Demetri GD, von Mehren M, Blanke CD, Van den Abbeele AD, Eisenberg B, Roberts PJ, et al. Efficacy and safety of imatinib mesylate in advanced gastrointestinal stromal tumors. N Engl J Med 2002;347:472–80.
7. Liegl B, Kepten I, Le C, Zhu M, Demetri G, Heinrich M, et al. Heterogeneity of kinase inhibitor resistance mechanisms in GIST. J Pathol 2008;216:64–74.
8. Demetri GD, Reichardt P, Kang Y-K, Blay J-Y, Rutkowski P, Gelderblom H, et al. Efficacy and safety of regorafenib for advanced gastrointestinal stromal tumours after failure of imatinib and sunitinib (GRID): an international, multicentre, randomised, placebo-controlled, phase 3 trial. Lancet 2013;381:295–302.
9. Demetri GD, van Oosterom AT, Garrett CR, Blackstein ME, Shah MH, Verweij J, et al. Efficacy and safety of sunitinib in patients with advanced gastrointestinal stromal tumour after failure of imatinib: a randomised controlled trial. Lancet 2006;368:1329–38.
10. Zhu MJ, Ou WB, Fletcher CDM, Cohen PS, Demetri GD, Fletcher JA. KIT oncoprotein interactions in gastrointestinal stromal tumors: therapeutic relevance. Oncogene 2007;26:6386–95.
11. Duensing A, Medeiros F, McConarty B, Joseph NE, Panigrahy D, Singer S, et al. Mechanisms of oncogenic KIT signal transduction in primary gastrointestinal stromal tumors (GISTs). Oncogene 2004;23:3999–4006.
12. Bauer S, Duensing A, Demetri GD, Fletcher JA. KIT oncogenic signaling mechanisms in imatinib-resistant gastrointestinal stromal tumor: PI3-kinase/AKT is a crucial survival pathway. Oncogene 2007;26:7560–8.
13. Bosbach B, Rossi F, Yozgat Y, Loo J, Zhang JQ, Berrozpe G, et al. Direct engagement of the PI3K pathway by mutant KIT dominates oncogenic signaling in gastrointestinal stromal tumor. Proc Natl Acad Sci U S A 2017;114:E8448–57.
14. Van Looy T, Wozniak A, Floris G, Sciot R, Li H, Wellens J, et al. Phosphoinositide 3-kinase inhibitors combined with imatinib in patient-derived xenograft models of gastrointestinal stromal tumors: rationale and efficacy. Clin Cancer Res 2014;20:6071–82.
15. Floris G, Wozniak A, Sciot R, Li H, Friedman L, Van Looy T, et al. A potent combination of the novel PI3K inhibitor, GDC-0941, with imatinib in gastrointestinal stromal tumor xenografts: long-lasting responses after treatment withdrawal. Clin Cancer Res 2013;19:620–30.
16. Dolly SO, Wagner AJ, Bendell JC, Kindler HL, Krug LM, Seiwert TY, et al. Phase I study of apitolisib (GDC-0980), dual phosphatidylinositol-3-kinase and mammalian target of rapamycin kinase inhibitor, in patients with advanced solid tumors. Clin Cancer Res 2016;22:2874–84.
17. NIH/U.S. National Library of Medicine. A dose-finding study of a combination of imatinib and BKM120 in the treatment of 3rd line GIST patients. Available from: https://clinicaltrials.gov/ct2/show/NCT01468688?term=PI3K&cond=GIST&rank=1.
18. NIH/U.S. National Library of Medicine. A dose-finding study of a combination of imatinib and BYL719 in the treatment of 3rd line GIST patients. Available from: https://clinicaltrials.gov/ct2/show/NCT01735968?term=PI3K&cond=GIST&rank=2.
19. Liu N, Rowley BR, Bull CO, Schneider C, Haegebarth A, Schatz CA, et al. BAY 80-6946 is a highly selective intravenous PI3K inhibitor with potent p110α and p110δ activities in tumor cell lines and xenograft models. Mol Cancer Ther 2013;12:2319–30.
20. Elster N, Cremona M, Morgan C, Toomey S, Carr A, O'Grady A, et al. A preclinical evaluation of the PI3K alpha/delta dominant inhibitor BAY 80-6946 in HER2-positive breast cancer models with acquired resistance to the HER2-targeted therapies trastuzumab and lapatinib. Breast Cancer Res Treat 2015;149:373–83
21. Krause G, Hassenrück F, Hallek M. Copanlisib for treatment of B-cell malignancies: the development of a PI3K inhibitor with considerable differences to idelalisib. Drug Des Devel Ther 2018;12:2577–90.

22. Okabe S, Tanaka Y, Tauchi T, Ohyashiki K. Copanlisib, a novel phosphoinositide 3-kinase inhibitor, combined with carfilzomib inhibits multiple myeloma cell proliferation. Ann Hematol 2019;98:723–33.
23. Patnaik A, Appleman LJ, Tolcher AW, Papadopoulos KP, Beeram M, Rasco DW, et al. First-in-human phase I study of copanlisib (BAY 80-6946), an intravenous pan-class I phosphatidylinositol 3-kinase inhibitor, in patients with advanced solid tumors and non-Hodgkin's lymphomas. Ann Oncol 2016;27:1928–40.
24. Dreyling M, Santoro A, Mollica L, Leppä S, Follows GA, Lenz G, et al. Phosphatidylinositol 3-kinase inhibition by copanlisib in relapsed or refractory indolent lymphoma. J Clin Oncol 2017;35:3898–905.
25. Copanlisib produces prolonged responses in lymphoma. Cancer Discov 2017; 7:OF2.
26. Serrano C, Mariño-Enríquez A, Tao DL, Ketzer J, Eilers G, Zhu M, et al. Complementary activity of tyrosine kinase inhibitors against secondary kit mutations in imatinib-resistant gastrointestinal stromal tumours. Br J Cancer 2019;120:612–20.
27. Will M, Qin ACR, Toy W, Yao Z, Rodrik-Outmezguine V, Schneider C, et al. Rapid induction of apoptosis by PI3K inhibitors is dependent upon their transient inhibition of RAS-ERK signaling. Cancer Discov 2014;4:334–47.
28. Yan H, Zhang B, Li S, Zhao Q. A formal model for analyzing drug combination effects and its application in TNF-α-induced NFκB pathway. BMC Syst Biol 2010;4:50.
29. Morschhauser F, Machiels J-P, Salles G, Rottey S, Rule SAJ, Cunningham D, et al. On-target pharmacodynamic activity of the PI3K inhibitor copanlisib in paired biopsies from patients with malignant lymphoma and advanced solid tumors. 2020;19:468–78.
30. Zook P, Pathak HB, Belinsky MG, Gersz L, Devarajan K, Zhou Y, et al. Combination of imatinib mesylate and AKT inhibitor provides synergistic effects in preclinical study of gastrointestinal stromal tumor. Clin Cancer Res 2017;23:171–80.
31. Conley AP, Araujo D, Ludwig J, Ravi V, Samuels BL, Thall HCF, et al. A randomized phase II study of perifosine (P) plus imatinib for patients with imatinib-resistant gastrointestinal stromal tumor (GIST). J Clin Oncol 27:15s, 2009 (suppl; abstr 10563).
32. Schöffski P, Reichardt P, Blay JY, Dumez H, Morgan JA, Ray-coquard I, et al. A phase I-II study of everolimus (RAD001) in combination with imatinib in patients with imatinib-resistant gastrointestinal stromal tumors. Ann Oncol 2010;21:1990–8.
33. Gordon PM, Fisher DE.Role for the proapoptotic factor BIM in mediating imatinib-induced apoptosis in a c-KIT-dependent gastrointestinal stromal tumor cell line. J Biol Chem 2010;285:14109–14.
34. Ran L, Sirota I, Cao Z, Murphy D, Chen Y, Shukla S, et al. Combined inhibition of MAP kinase and KIT signaling synergistically destabilizes ETV1 and suppresses GIST tumor growth. Cancer Discov 2015;5:304–15.
35. Garner AP, Gozgit JM, Anjum R, Vodala S, Schrock A, Zhou T, et al. Ponatinib inhibits polyclonal drug-resistant KIT oncoproteins and shows therapeutic potential in heavily pretreated gastrointestinal stromal tumor (GIST) patients. Clin Cancer Res 2014;20:5745–55.
36. Smith BD, Kaufman MD, Lu W-P, Gupta A, Leary CB, Wise SC, et al. Ripretinib (DCC-2618) is a switch control kinase inhibitor of a broad spectrum of oncogenic and drug-resistant KIT and PDGFRA variants. Cancer Cell 2019; 35:738–751.
37. Yu Y, Yoon S-O, Poulogiannis G, Yang Q, Ma XM, Villen J, et al. Phosphoproteomic analysis identifies Grb10 as an mTORC1 substrate that negatively regulates insulin signaling. Science 2011;332:1322–6.
38. Sarbassov DD, Guertin DA, Ali SM, Sabatini DM. Phosphorylation and regulation of Akt/PKB by the rictor-mTOR complex. Science 2005;307: 1098–101.
39. Janku F, Yap TA, Meric-Bernstam F. Targeting the PI3K pathway in cancer: are we making headway? Nat Rev Clin Oncol 2018;15:273–91.